9-2012

A first-principles molecular dynamics approach for predicting optical phonon lifetimes and far-infrared reflectance of polar materials

Hua Bao
Purdue University, hbao@purdue.edu

Bo Qiu
Purdue University, qiub3@purdue.edu

Yu Zhang
Purdue University, zhan1219@purdue.edu

Xiulin Ruan
Purdue University, ruan@purdue.edu

Follow this and additional works at: http://docs.lib.purdue.edu/nanopub

 Part of the Nanoscience and Nanotechnology Commons

A first-principles molecular dynamics approach for predicting optical phonon lifetimes and far-infrared reflectance of polar materials

Hua Bao [a], Bo Qiu [a], Yu Zhang [b], Xiulin Ruan [a,*]

[a] School of Mechanical Engineering and Birck Nanotechnology Center, Purdue University, West Lafayette, IN 47907, United States
[b] Department of Chemistry, University of California, Irvine, CA 92697, United States

ARTICLE INFO

ABSTRACT

The Lorentz oscillator model is well-known for its effectiveness to describe the far-infrared optical properties of polar materials. The oscillator strength and damping factor in this model are usually obtained by fitting to experimental data. In this work, a method based on first-principles simulations is developed to parameterize the Lorentz oscillator model without any fitting parameters. The high frequency dielectric constant is obtained from density functional perturbation theory, while the optical phonon frequencies and damping factors are calculated using an analysis of *ab initio* molecular dynamics trajectories. This method is then used to predict the far-infrared properties of GaAs, and the results are in good agreement with experimental data.

© 2012 Elsevier Ltd. All rights reserved.

1. Introduction

Far-infrared optical property is a basic material property that is important for many applications, such as atomic structure identification [1,2], thermal radiation transfer [3,4], and metamaterials [5,6]. Many efforts have been devoted to obtain a thorough understanding of the interaction between far-infrared electromagnetic waves and materials. It has been well known that the dielectric response within far-infrared spectrum in solids is due to the coupling of electromagnetic waves with free electrons and charged ions [7]. Free electron absorption is the dominating mechanism in metals and doped semiconductors, and the dielectric function can be well-described by the Drude free electron model [8]. Charged ion absorption, in contrast, is due to lattice vibrations and bound electrons. It is the dominating absorption mechanism in dielectric and pure (or lightly doped) semiconductor materials.

Ion-induced infrared absorption of a material is usually described by the Lorentz oscillator model, in which it is assumed that charged ions are oscillating driven by external electric fields [7]. Ion displacements can thus be obtained by solving the equation of motion of a damped oscillator. As a result, the frequency-dependent dielectric function $\varepsilon(\omega)$ of a polar material in the far-infrared regime can usually be written in the following form [7]:

$$\varepsilon(\omega) = \varepsilon(\infty) + \sum_m \frac{S_m \omega_m^2}{\omega_m^2 - \omega^2 - i\gamma_m \omega}, \qquad (1)$$

where $\varepsilon(\infty)$ denotes the high frequency dielectric constant, ω denotes the angular frequency, γ is the damping factor, S denotes the oscillator strength, and m goes over all the resonant frequencies in the system. Unlike the Drude free electron model, the parameters in the Lorentz oscillator model, especially the damping factor, are generally difficult to predict from theory [9], and they are often treated as adjustable parameters and determined by

fitting to experimental results. Some previous studies have attempted to parameterize the Lorentz model from first principles [10,11], in which the density functional perturbation theory (DFPT) is usually applied to calculate oscillator frequencies and the damping factor is usually neglected ($\gamma_m = 0$). The results can only be used to determine the positions of infrared reflection peaks at zero temperature. The temperature-dependent peak shift cannot be captured and the value of the reflectance in the resonant region always goes to one (total reflection) due to the neglecting of damping factor. Another method based on fluctuation–dissipation theory was also employed to predict the infrared absorption [12,13,4], in which the imaginary part of the dielectric function ε_2 was determined by the Fourier transform of the autocorrelation function (ACF) of the total dielectric polarization. This method is based on molecular dynamics (MD) simulations and applicable at different temperatures. However, it is not simple to use this method in practice. If first-principles MD is used [12,13], the calculation of polarization is quite computationally demanding, so the results can only be obtained for a short time period. A Fourier transform of the ACF will not provide enough resolution in the frequency domain to resolve the absorption peaks in the spectra. If classical MD is used, the accuracy of the empirical potential is always a concern. It is generally quite difficult to develop an empirical potential that can accurately predict the dielectric polarization, as well as the optical phonon properties.

In this work, we report a method that can parameterize the Lorentz oscillator model and predict the far-infrared optical property from first principles. The relationship between the Lorentz oscillator model and the properties of the infrared-active optical phonons is first discussed. First-principles methods are then proposed to calculate parameters in the Lorentz oscillator model. The far-infrared reflectance of GaAs is predicted to demonstrate this method and the results are compared with experiments.

2. Theory and methodology

2.1. Theory

The resonant modes in Eq. (1) in a polar material are associated with its phonon modes. Because photons have negligible momentum compared to phonons, only certain phonon modes with very small momentum (zone-center) can interact with infrared photons. In another point of view, the electromagnetic waves only interact with those phonon modes that induce polarizations. To establish a relationship between the parameters and Eq. (1) and the phonon properties, we follow Born and Huang's phenomenological theory [14] and consider a diatomic ionic material with cubic lattice. The masses of positive and negative ions are denoted by M_+ and M_-, and the displacements are $\mathbf{u}_+$ and $\mathbf{u}_-$. The $\mathbf{w}$ parameter is defined as

$$\mathbf{w} = \left(\frac{\overline{M}}{\Omega}\right)^{1/2} (\mathbf{u}_+ - \mathbf{u}_-), \tag{2}$$

where $\overline{M} = M_+ M_- / (M_+ + M_-)$ is the reduced mass, and Ω is the volume of a unit cell. The following equations are then introduced:

$$\mathbf{P} = b_{21}\mathbf{w} + b_{22}\mathbf{E}, \tag{3}$$

$$\ddot{\mathbf{w}} = b_{11}\mathbf{w} - \gamma\dot{\mathbf{w}} + b_{12}\mathbf{E}, \tag{4}$$

where $\mathbf{E}$ is the external electric field, $\mathbf{P}$ is the macroscopic polarization, b_{11}, b_{12}, b_{21}, b_{22} are coefficients determined by the properties of the specific material, including Born effective charge, polarizability of the atoms, reduced mass, force constant between positive and negative ions, etc. [14]. The definition of dielectric function is given by

$$\varepsilon(\omega) = \frac{\varepsilon_0 \mathbf{E} + \mathbf{P}}{\varepsilon_0 \mathbf{E}}, \tag{5}$$

where ε_0 is the dielectric permittivity of the vacuum. Combining Eqs. (3)–(5), Born and Huang showed that [14]

$$\frac{\varepsilon(\omega)}{\varepsilon(\infty)} = 1 + \frac{\omega_0^2(\varepsilon(0) - \varepsilon(\infty))}{\omega_0^2 - \omega^2 - i\omega\gamma}, \tag{6}$$

where $\omega_0^2 = b_{11}$. If no external driving electric field is applied, i.e., $\mathbf{E} = 0$, the solution of Eq. (4) will be

$$\mathbf{w} = \mathbf{A}e^{-\gamma t/2} \cos(\omega_1 t), \tag{7}$$

where $\mathbf{A}$ is a constant and $\omega_1 = (\omega_0^2 - \gamma^2/4)^{1/2}$. Considering that damping factor γ is usually much smaller than ω_0, so it can be approximated that $\omega_1 \approx \omega_0$.

On the other hand, under the relaxation time approximation, the zone-center transverse optical (TO) phonon vibration can be written as [15]

$$q_{TO} = \mathbf{B}e^{-\Gamma t} \cos(\omega_{TO} t), \tag{8}$$

where $\mathbf{B}$ and Γ are the amplitude and the linewidth of the TO phonon mode, respectively. The phonon linewidth Γ is related to the phonon lifetime τ by $\Gamma = 1/(2\tau)$. It can be seen that $\mathbf{w}$ is proportional to the magnitude of the zone-center TO phonon mode, by noting that zone-center TO phonon is the relative motion of the ions in one unit cell. Therefore, $\mathbf{w}$ and q_{TO} are actually equivalent (differ by no more than a constant). Comparing Eqs. (7) and (8), it can be concluded that $\omega_{TO} \approx \omega_0$ and $\Gamma = \gamma/2$. Considering the equations above and the Lyddane–Sachs–Teller (LST) relationship [16]

$$\frac{\omega_{LO}}{\omega_{TO}} = \left[\frac{\varepsilon(0)}{\varepsilon(\infty)}\right]^{1/2}, \tag{9}$$

where LO denotes longitudinal optical (phonon) and $\varepsilon(0)$ is the static dielectric constant. Eq. (6) can be rewritten as

$$\frac{\varepsilon(\omega)}{\varepsilon(\infty)} = 1 + \frac{\omega_{LO}^2 - \omega_{TO}^2}{\omega_{TO}^2 - \omega^2 - i(2\Gamma)\omega}. \tag{10}$$

Therefore, to parameterize this equation, one simply needs to obtain the high frequency dielectric constant $\varepsilon(\infty)$, infrared active TO phonon frequencies ω_{TO} and corresponding LO phonon frequencies ω_{LO}, and the linewidth Γ of the infrared active TO phonons. It should be pointed out that the relationship between damping factor and TO phonon linewidth can be generalized to other lattice structures with more than one infrared-active phonon modes [17,18]. If the generalized LST relationship [11,16] is applied and the mode

coupling is neglected, Eq. (10) can be generalized to a multimode Lorentz oscillator model.

2.2. Method

The high frequency dielectric function and phonon frequencies can be calculated based on DFPT [19], as used in our previous work [10]. For the prediction of the phonon relaxation time, so far several methods have been developed, including the perturbation method [20], normal mode analysis (NMA) [21–23], and the spectral energy density (SED) analysis [24–27]. The perturbation method is used in the frequency domain, which uses Fermi's golden rule to calculate the three-phonon scattering rates resulted from lattice anharmonicity. It is generally limited to bulk materials with perfect translational symmetry and can usually only include first-order anharmonicity. Also, the temperature effect can only be implicitly included by tuning the phonon occupation number based on a zero-temperature phonon density of states [20]. The latter two methods map the MD trajectory to each individual phonon normal modes, and then derive the spectral phonon relaxation time from either the phonon population decay in the time domain or the phonon linewidth in the frequency domain. It should be noted that recent SED studies have only used the atomic velocity data to predict phonon relaxation times [24–26]. In those papers, the SED was defined as

$$\Phi'(\boldsymbol{\kappa},\omega) = \frac{1}{4\pi\tau_0 N} \sum_j^N m_j \sum_\alpha^3 \left| \int_{-\tau_0}^{\tau_0} \dot{u}_{j,\alpha}(t) \exp(i\boldsymbol{\kappa}\cdot\mathbf{r}_j - i\omega t)\, dt \right|^2, \tag{11}$$

where ω is the angular frequency, $\boldsymbol{\kappa}$ is the phonon wave vector, N is the total number of atoms, m_j is the mass of atom j, α denotes the three spatial components, u_j and $\dot{u}_j$ are the displacement and velocity of atom j, and $\mathbf{r}_j$ is the equilibrium position of atom j. The phonon frequencies and relaxation times were obtained from the peak location and peak width of Φ'. However, it was later pointed out by Larkin et al. that the polarization vector should also be included in the formulation of SED functions in order to predict the phonon relaxation time, and the formulation of SED in Eq. (11) can only be used to predict phonon frequencies [27]. In the new SED formulation, the instant normal mode of a phonon wave vector $\boldsymbol{\kappa}$ and phonon branch index v can be written as

$$q\binom{\boldsymbol{\kappa}}{v}; t) = N^{-1/2} \sum_j m_j^{1/2} \exp(i\boldsymbol{\kappa}\cdot\mathbf{r}_j) \mathbf{e}^*\binom{\boldsymbol{\kappa}}{v} \cdot \mathbf{u}_j(t), \tag{12}$$

where $\mathbf{e}\binom{\boldsymbol{\kappa}}{v}$ is the mode polarization and the asterisk superscript denotes the complex conjugate. The average kinetic energy in the frequency domain is

$$\langle E_k\binom{\boldsymbol{\kappa}}{v};\omega) \rangle = \lim_{\tau_0 \to \infty} \frac{1}{4\tau_0} \left| \frac{1}{\sqrt{2\pi}} \int_{-\tau_0}^{\tau_0} \dot{q}\binom{\boldsymbol{\kappa}}{v};t) \exp(-i\omega t)\, dt \right|^2, \tag{13}$$

where E_k is the kinetic energy and $\dot{q}$ is the time derivative of the normal mode. The new SED is

$$\Phi(\boldsymbol{\kappa},\omega) = 2 \sum_v^{3n} \langle E_k\binom{\boldsymbol{\kappa}}{v};\omega) \rangle, \tag{14}$$

where n is the number of atoms in a unit cell. The NMA method differs from SED because it extracts the phonon relaxation time in the time domain. It computes the total energy of each phonon mode [21]

$$E\binom{\boldsymbol{\kappa}}{v};t) = E_p\binom{\boldsymbol{\kappa}}{v};t) + E_k\binom{\boldsymbol{\kappa}}{v};t) \tag{15}$$

$$E\binom{\boldsymbol{\kappa}}{v};t) = \frac{\omega^2 q^*\binom{\boldsymbol{\kappa}}{v};t) q\binom{\boldsymbol{\kappa}}{v};t)}{2} + \frac{\dot{q}^*\binom{\boldsymbol{\kappa}}{v};t) \dot{q}\binom{\boldsymbol{\kappa}}{v};t)}{2}, \tag{16}$$

where E_p denotes potential energy. The phonon relaxation time is obtained by fitting the ACF of $E\binom{\boldsymbol{\kappa}}{v};t)$ to an exponential decay.

Comparing to the perturbation method, methods based on MD can give phonon frequency and relaxation time from a real-time simulation. Higher order anharmonic effects and temperature effects are naturally included, so the predicted phonon frequencies and linewidth should be more reliable. One can apply such method to high temperature and high pressure systems (such as the earth mantle [17]), which will be useful to study radiative heat transport at extreme conditions. In this work, the phonon frequencies and relaxation times are obtained by an analysis of MD trajectories (based on SED and NMA), but the classical MD is replaced by the *ab initio* MD [28]. It is necessary because the classical interatomic potentials usually fail to accurately predict optical phonon properties.

3. Simulation details

GaAs is used as an example to demonstrate this method. GaAs has a simple zinc-blende structure with two atoms in the primitive cell. There are two degenerate TO phonon branches and one LO phonon branch. The zone-center optical phonon is the only infrared active phonon mode in GaAs. The first-principles calculations are carried out with the VASP package [29], using the Ceperley–Alder exchange and correlation functional [30] and Vanderbilt ultrasoft pseudopotential [31]. The geometry is first relaxed to eliminate the internal stress, and the resulting optimized lattice constant is 5.597 Å (5.65 Å from the experiment [32]). A $2 \times 2 \times 2$ supercell containing 64 atoms is used for the phonon linewidth calculation and an $8 \times 1 \times 1$ cell is used for phonon dispersion calculations. For the $2 \times 2 \times 2$ supercell, only Γ point is used in the electron density integration, while for the $8 \times 1 \times 1$ cell four k-points are used. An 80 ps microcanonical trajectory is used for the phonon dispersion calculation and 160 ps trajectories are used for relaxation time calculations. An ionic step of 2 fs is used for all MD simulations.

4. Results and discussion

4.1. Phonon dispersion

The phonon dispersion curve at 300 K is first calculated based on the SED method. Since only phonon frequencies are of interest at this moment, Eq. (11) is used here due to the simplicity. The $8 \times 1 \times 1$ supercell allows us to extract nine k-points from Γ to X point in the
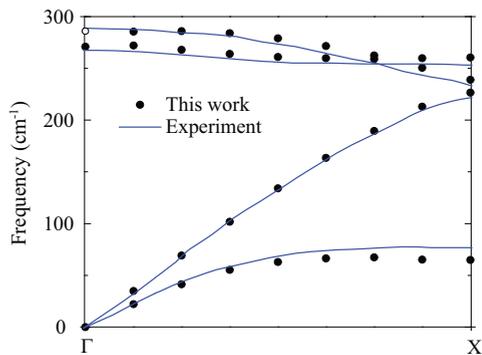
Fig. 1. The calculated phonon dispersion curve at 300 K and the phonon dispersion extracted by neutron scattering measurements at 295 K [33].

Fig. 2. (a) The Γ point SED of a 300 ps MD trajectory at 300 K, using a $2 \times 2 \times 2$ supercell. (b) The ACF of TO mode energy and the exponential fitting.
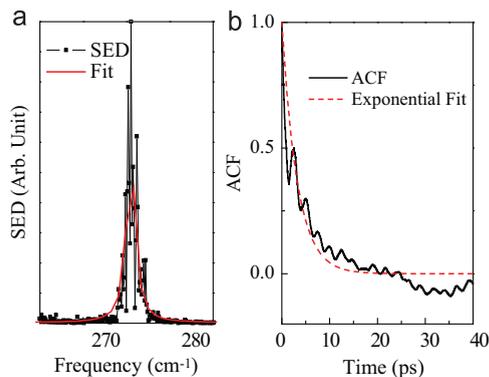
Table 1
Calculated zone-center TO and LO phonon frequencies compared to experimental results from neutron scattering and infrared reflectance measurements summarized in Ref. [33].

| Parameters	This work	Neutron	Infrared
ω_{TO}	271	267.5	268.2
ω_{LO}	286	285.2	291.5

first Brillouin zone, and the result is plotted in Fig. 1, together with the experimental results from a neutron scattering measurement [33]. It is clear that the predicted dispersion agrees with the experiment quite well. The zone-center TO and LO phonon frequencies are compared with experiments and listed in Table 1. It should be noted that the zone-center LO phonon cannot be directly captured by any MD simulations. The zone-center LO–TO splitting is due to the macroscopic electrical field induced by the long wavelength phonon vibration, which does not appear in SED because of the periodic boundary condition. The value in Table 1 is extrapolated from the LO phonon frequencies of adjacent k-points.

4.2. Phonon linewidth

Phonon linewidths can be directly obtained by fitting the SED spectra with Lorentz function, and the half-width at half-maximum will be the linewidth of the phonon mode. However, due to the large computational cost of *ab initio* MD, the MD trajectories can only be generated within a short time scale. As shown in Fig. 2(a), even for a 300 ps MD trajectory, the frequency domain resolution is still as large as 0.11 cm^{-1}. There are only a few data points within the peak (peak width is around 2 cm^{-1}), so the linewidth extracted with the peak fitting can have quite large uncertainty. Therefore, the NMA method is followed. For zone-center phonon mode of a diatomic material, the normal mode polarization vector **e** does not have to be calculated. By noting that the magnitude of this phonon mode is proportional to the difference of the displacements of positive charged and negative charged ion, the calculation can be further simplified by replacing
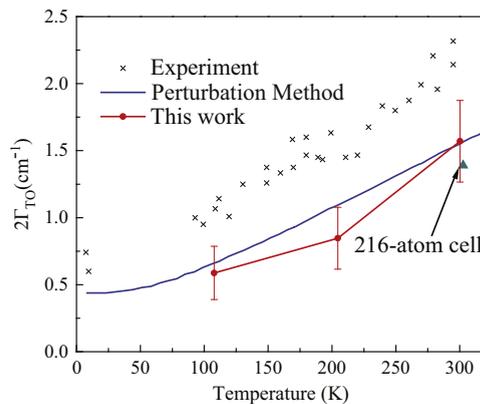
Fig. 3. A comparison of temperature-dependent linewidth of the TO phonon of GaAs: this work, the perturbation method [20], and the experimental data [34]. The error bars show the standard deviation of nine results from separated trajectories.

$q(t)$ in Eq. (12) with $[u_{+,\alpha}(t) - u_{-,\alpha}(t)]$, where α denotes the three components in space.

Using this method, the temperature-dependent TO phonon linewidth can be extracted. For each temperature, the ensemble average is achieved by averaging ACF of nine independent MD trajectories. The phonon linewidths at different temperatures are compared with previous calculations and experiments, as shown in Fig. 3. To be comparable with the existing data from the literature, 2Γ is shown. Also, one data point is obtained by a single MD trajectory at 300 K of a large $3 \times 3 \times 3$ supercell (216 atoms). The extracted phonon linewidth is similar to that from the $2 \times 2 \times 2$ cell. This indicates that the size effect of simulation domain is not significant, at least for GaAs. The linewidth increases as the temperature increases (the relaxation time is shorter at higher temperature), which can be explained by the increased phonon–phonon scattering at higher temperature. Our results show a good agreement with the results from the perturbation method. The discrepancy with experimental results can be attributed to the
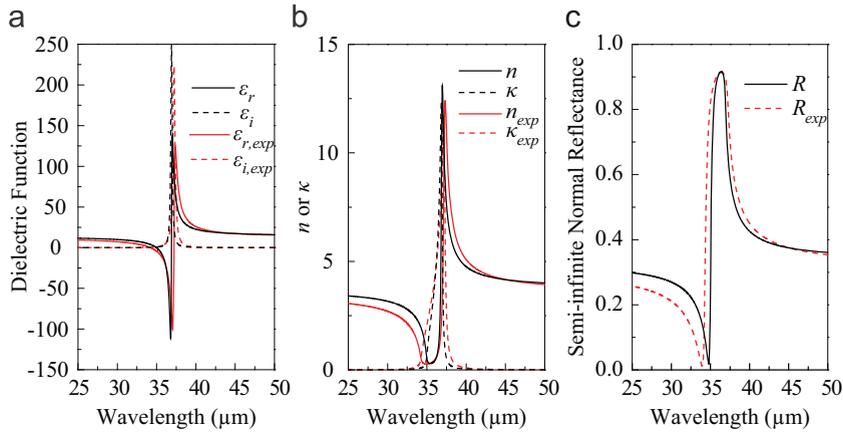
Fig. 4. The calculated (a) dielectric function, (b) refractive index, and (c) semi-infinite normal reflectance at 300 K and experimental results at 295 K (denoted by "exp") [35,36].

uncertainties in the experiments: for example, defects, dopants, material surfaces, and thermal excited free electrons can all induce additional broadening of phonon linewidth. It should be pointed out that the predicted phonon linewidth does not show the expected improvement comparing to the results of the perturbation method in this case. It is possible that the lattice of GaAs in this temperature range is harmonic enough so that only including the third order energy derivative is enough to describe lattice anharmonicity. It requires further investigation to determine under what conditions our method based on MD is better than the perturbation method. In spite of that, this work validates the *ab initio* MD simulations to predict the relaxation times of phonons. To the best knowledge of the authors, this work is the first use of such a method to parameterize the Lorenz oscillator model and predict infrared radiative properties.

4.3. Semi-infinite normal reflectance

The calculation of high frequency dielectric function was performed in our previous work [10]. To keep this work fully *ab initio*, we used the high frequency dielectric function of $\varepsilon_\infty = 12.85$ from that work. Combining it with $\omega_{TO} = 271$ cm^{-1}, $\omega_{LO} = 286$ cm^{-1}, and $\gamma = 2\Gamma_{TO} = 1.59$ cm^{-1}, the Lorentz oscillator model in Eq. (10) is fully parameterized. The semi-infinite normal reflectance in the Reststrahlen band can then be calculated using the following equations:

$$\varepsilon = (n + i\kappa)^2, \tag{17}$$

$$R = \left| \frac{n - 1 + i\kappa}{n + 1 + i\kappa} \right|^2, \tag{18}$$

where n and κ are the real and imaginary parts of the refractive index and R is the normal reflectance. The calculated refractive index and reflectance are compared with experimental results, as shown in Fig. 4. Our calculation matches the experimental results quite well, considering all the parameters are calculated based on first principles.

5. Summary

In summary, this work has established the relationship between the parameters in the Lorentz oscillator model and the properties of infrared active phonon modes. A method based on first principles is then developed to parameterize the Lorentz oscillator model and predict the far-infrared radiative properties of polar materials. The TO phonon frequency and corresponding linewidth are extracted from the analysis *ab initio* MD trajectories. The LO phonon frequency is obtained by extrapolating the phonon dispersion curve predicted by SED. The infrared reflectance of GaAs is then calculated by parameterizing the Lorentz oscillator model and an overall good agreement with experiments is seen.

References

[1] Acik M, Lee G, Mattevi C, Chhowalla M, Cho K, Chabal YJ. Nat Mater 2010;9:840.
[2] Luo G, Li H, Wang L, Lai L, Zhou J, Qin R, et al. J Phys Chem C 2010;114:6959.
[3] Gentle AR, Smith GB. Nano Lett 2010;10:373.
[4] Adebayo GA, Liang Y, Miranda CR, Scandolo S. J Chem Phys 2009;131:014506.
[5] Wang LP, Zhang ZM. Opt Express 2010;19:A126.
[6] Vassand S, Marquier F, Greffet JJ, Pardo F, Pelouard JL. Appl Phys Lett 2010;97:161101.
[7] Zhang ZM. Nano/microscale heat transfer. New York: McGraw-Hill; 2007.
[8] Drude P. Ann Phys 1900;306:566.
[9] Zhang ZM, Fu CJ, Zhu QZ. Adv Heat Transfer 2003;37:179.
[10] Bao H, Ruan XL. Int J Heat Mass Transfer 2010;53:1308.
[11] Lee K, Pickett WE. Phys Rev B 2003;68.

[12] Debernardi A, Bernasconi M, Cardona M, Parrinello M. Appl Phys Lett 1997;71:2692.
[13] Bernasconi M, Silvestrelli PL, Parrinello M. Phys Rev Lett 1998;81: 1235.
[14] Born M, Huang K. Dynamical theory of crystal lattice. Oxford: Oxford University Press; 1954.
[15] Ladd AJC, Moran B, Hoover WG. Phys Rev B 1986;34:5058.
[16] Burns G. Solid state physics. Orlando: Academic Press; 1985.
[17] Hofmeister AM. Science 1999;283:1699.
[18] Hofmeister AM. Am Mineral 2001;86:1188.
[19] Martin R. Electronic structure: basic theory and practical methods. Cambridge, UK: Cambridge University Press; 2004.
[20] Debernardi A. Phys Rev B 1998;57:12847.
[21] McGaughey A, Kaviany M. Phys Rev B 2004;69(1):094303.
[22] Shiomi J, Maruyama S. Phys Rev B 2006;73:205420.
[23] Henry AS, Chen G. J Comput Theor Nanosci 2008;5:141.
[24] de Koker N. Phys Rev Lett 2009;103:125902.
[25] Thomas JA, Turney JE, Iutzi RM, Amon CH, McGaughey AJH. Phys Rev B 2010;81:081411.
[26] Qiu B, Bao H, Zhang G, Wu Y, Ruan X. Comput Mater Sci 2012;53: 278.
[27] Larkin JM, Massicotte AD, Turney JE, McGauphey AJH, Amon CH. In: 2012 ASME micro/nanoscale heat and mass transfer international conference. Atlanta, GA; March 2012.
[28] Car R, Parrinello M. Phys Rev Lett 1985;55:2471.
[29] Kresse G, Furthmuller J. Comput Mater Sci 1996;6:15.
[30] Ceperley DM, Alder BJ. Phys Rev Lett 1980;45:566.
[31] Vanderbilt D. Phys Rev B 1990;41.
[32] Kittel C. Introduction to solid state physics. New York: John Wiley; 1996.
[33] Blakemore J. J Appl Phys 1982;53:R123.
[34] Irmer G, Wenzel M, Monecke J. Phys Status Solidi B 1996;195:85.
[35] Lockwood DJ, Yu G, Rowell NL. Solid State Commun 2005;136:404.
[36] Palik E. Handbook of optical constants of solids. Elsevier; 1998.